Risbey, J. S., Grose, M. R., Monselesan, D. P., O'Kane, T. J., & Lewandowsky, S. (2017). Transient response of the global mean warming rate and its spatial variation. *Weather and Climate Extremes*, *18*, 55-64. https://doi.org/10.1016/j.wace.2017.11.002

Weather and Climate Extremes 18 (2017) 55–64

Contents lists available at ScienceDirect

Weather and Climate Extremes

journal homepage: www.elsevier.com/locate/wace

Transient response of the global mean warming rate and its spatial variation

James S. Risbey [a,*], Michael R. Grose [a], Didier P. Monselesan [a], Terence J. O'Kane [a], Stephan Lewandowsky [a,b,c]

[a] CSIRO Oceans & Atmosphere, Hobart, Australia
[b] University of Bristol, Bristol, UK
[c] University of Western Australia, Perth, Australia

ARTICLE INFO

Keywords:
Climate variability
Climate projection
Transient response
Extreme warming

ABSTRACT

The Earth has warmed over the past century. The warming rate (amount of warming over a given period) varies in time and space. Observations show a recent increase in global mean warming rate, which is initially maintained in model projections, but which diverges substantially in future depending on the emissions scenario followed. Scenarios that stabilize forcing lead to much lower warming rates, as the rate depends on the change in forcing, not the amount. Warming rates vary spatially across the planet, but most areas show a shift toward higher warming rates in recent decades. The areal distribution of warming rates is also changing shape to include a longer tail in recent decades. Some areas of the planet are already experiencing extreme warming rates of about 1 °C/decade. The fat tail in areal distribution of warming rates is pronounced in model runs when the forcing and global mean warming rate is increasing, and indicates a climate state more prone to regime transitions. The area-proportion of the Earth displaying warming/cooling trends is shown to be directly related to the global mean warming rate, especially for trends of length 15 years and longer. Since the global mean warming rate depends on the forcing rate, the proportion of warming/cooling trend areas in future also depends critically on the choice of future forcing scenario.

1. Introduction

The Earth is undergoing long term warming in response to increases in greenhouse gas concentrations in the atmosphere (Houghton et al., 1990). The warming can be characterised by the total change or *amount* of warming from a base period (usually pre-industrial), and by the *rate* of change of warming over a specified interval of time. Both the *amount* and *rate* of warming are important variables for adaptation to climate change. This is because some species, ecosystems, crops, or sectors of the economy are sensitive to the actual temperature (and therefore amount of change), and some are sensitive to the rate of change because of the need to migrate or adapt to maintain similar environments as temperatures change (Thomas et al., 2004; Quintero and Wiens, 2013; Oppenheimer et al., 2014; Burke et al., 2015). So far there has been more attention in the climate community to quantifying the *amount* than *rate* of warming.

The rate of global mean surface warming (warming rate) has increased in the modern period (since about 1970) (Stocker et al., 2013; Lewandowsky et al., 2015; Hansen et al., 2012). The transient response of the climate system is not uniform in space or time (Schneider and Thompson, 1981). The global mean surface temperature (GMST) exhibits fluctuations in time, where some decades warm more rapidly than others (Houghton et al., 1990; Marotzke and Forster, 2015; Risbey, 2015). The processes responsible for variation in warming rate through time (on time scales shorter than the greenhouse response of many decades and longer) include natural internal variability of the coupled climate system and changes in external forcing associated with variable solar forcing and aerosol loading (Houghton et al., 1990). Such variations always occur and are evident in Fig. 1a throughout the instrumental record. This work addresses variations in the warming rate through time in observations and projections of the rate in models.

We also examine the degree to which the warming rate is uniformly expressed in space. There is considerable regional (spatial) heterogeneity in the warming (Hansen et al., 2012; Sutton et al., 2015). There are good reasons why all regions of the Earth do not warm at the same rate. These include:

Land/ocean contrast: It is well known that the oceans, with higher heat capacity and the ability to store heat, respond more sluggishly than the land regions (Schneider and Thompson, 1981).

* Corresponding author. CSIRO Oceans & Atmosphere, Box 1538, Hobart, Tas 7001, Australia.
E-mail address: james.risbey@csiro.au (J.S. Risbey).

https://doi.org/10.1016/j.wace.2017.11.002
Received 23 July 2016; Received in revised form 14 November 2017; Accepted 15 November 2017
Available online 26 November 2017

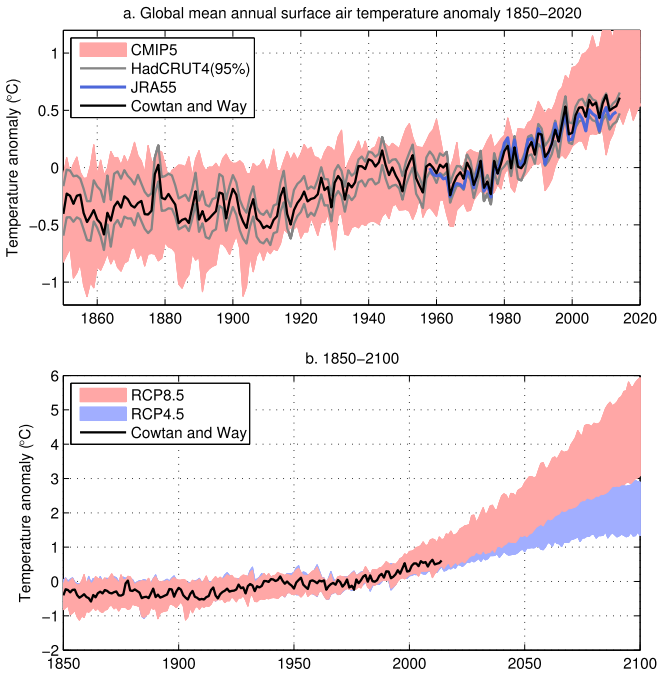

Fig. 1. Global mean surface temperature series a) for HadCRUT4 observations (grey), JRA55 reanalysis (blue), Cowtan and Way (black) and the 2.5–97.5 percentile distribution from the CMIP5 historical and RCP8.5 series; b) projections of GMST to 2100 for the CMIP5 2.5–97.5 percentile distribution in RCP4.5 (blue) and RCP8.5 (red), with Cowtan & Way observations (black).

Ocean circulation: Persistent ocean currents may keep some regions cooler or warmer than the average. Changes in ocean circulation will change the distribution of regions with different heating rates (Held, 1993).

Atmospheric circulation: Meridional (north-south) flows in the atmosphere are induced by persistent blocking modes (O'Kane et al., 2013, 2016). Changes in the locations of preferred blocking regions over decades can change warm/cold advection over a region, changing the local rate of warming.

Cryosphere response: Changes in the cryosphere in high latitudes through changes in albedo, sea ice, and meltwater can change the surface temperature, lapse rate, and meridional temperature gradient, which can induce local and larger scale changes in warming rate (Hansen and Takahashi, 1984; Held, 1993).

Heterogeneous radiative forcing: Atmospheric radiative forcing differs from one region to another due to differences in aerosol loading and distributions of some trace gases (Ramanathan et al., 1987; Ramaswamy et al., 2001).

Given the clear reasons for differences in regional warming rates, one should not expect all regions to warm together. Relevant questions are: what is the distribution of warming rates in space, and how much of the Earth is undergoing warming at any given point in time. The latter question is relevant to how strongly one can generalise regional expectations from the global mean (Grenier et al., 2015). If a region shows little or no warming, is that unusual and what does that imply in evaluating climate projections? (Grose et al., 2017). We do not explore specific regional responses here as that is done elsewhere (Grenier et al., 2015; Sutton et al., 2015; Grose et al., 2017).

2. Data and methods

A range of different data sets are used here to represent GMST. For instrumental data, we use HadCRUT4 (Morice et al., 2012); Cowtan and Way (2014), and GISTEMP (Hansen et al., 2010). In some cases we also compare this data with GMST from the NCEP-NCAR 20th century reanalysis (Compo et al., 2011) and the JRA55 reanalysis (Kobayashi et al., 2015). The reanalyses are used to provide gridded surface temperature, along with Cowtan & Way. Cowtan & Way is a conservative choice because it relies on HadSST3, which shows slower warming than the ERSSTv4 and COBE-SST version 2 reconstruction (Kent et al., 2017; Hausfather et al., 2017).

We calculate a number of diagnostics here based on spatial analyses of surface temperature in gridded surface temperature datasets. Our purposes are best served by a surface temperature dataset with fuller spatial coverage using optimal interpolation. Among the most complete datasets in this regard is Cowtan & Way, who have used a kriging method for optimal interpolation to provide gridded data back to 1850, from which we can do spatial analyses (calculate area proportions showing warming/cooling in given periods). While other surface temperature datasets also provide gridded data, they have not all provided the same focus on data coverage and interpolation procedures needed to minimise the consequences of missing data cells through the earlier part of the temperature record.

The sparser data in the earlier part of the temperature record is potentially an issue for the kinds of spatial analysis carried out here. To provide a measure of this uncertainty we have employed different datasets and different types of data in the analysis. For example, we repeated all analyses here with the 20th century reanalysis, which is a gridded product with full grids through the earlier period like Cowtan & Way. The 20th century reanalysis is perhaps regarded as a less reliable product for surface air temperature than dedicated instrumental products because it relies on model reanalysis with surface and atmospheric data. Despite this, the results for the 20th century reanalysis are qualitatively similar with relatively minor quantitative differences for the analyses presented here. This increases our confidence that the larger uncertainties in the earlier part of the record for the spatial analyses are probably not critical for the outcomes shown.

GMST is also taken from Coupled Model Intercomparison Project (CMIP5) models (Taylor et al., 2012) with one run per model generating a multi-model ensemble. Note that for the CMIP5 models we use surface air temperature to represent GMST, which is different from the observed GMST records that contain a blend of surface air temperatures over land and sea surface temperatures over ocean. Over the recent instrumental period, this introduces a slight underestimate of temperature changes in the observed GMST series (Cowtan et al., 2015).

The CMIP5 ensemble is typically represented here by a band covering the 2.5–97.5 percentile range of results. The CMIP5 ensemble runs span 1850–2100, with historical forcing for the period 1850–2005, and Representative Concentration Pathway (RCP) RCP2.6, RCP4.5, and RCP8.5 (Moss et al., 2010) forcing from 2006 to 2100. The number of model runs varies depending on the RCP used and is 22, 27, and 32 for RCP 2.6, 4.5, and 8.5 respectively. The profile of each of the RCP scenarios is shown in Fig. 2 and corresponds to a complete phase out of greenhouse gas emissions and an arrest in the forcing increase for RCP2.6, eventual reduction in greenhouse emissions and a stabilisation of forcing at a higher level for RCP4.5, and continued rise in greenhouse emissions and radiative forcing to much higher levels for RCP8.5.

The response of GMST to the RCP 4.5 and 8.5 forcings is shown in Fig. 1b for the period out to 2100. The response is fairly similar through about 2020, and then the RCP8.5 scenario exhibits faster warming. For the RCP4.5 scenario the forcing stabilizes (Fig. 2) and the rate of warming eventually decreases, as shown by the reduction in gradient of the blue envelope near the end of the series in Fig. 1b and in section 3.1. In some cases we wish to illustrate variability in the CMIP5 model runs more specifically than in the collective ensemble. In that case we use either the ACCESS1.0 model (Dix & coauthors, 2013) or the CCSM4 (Gent et al., 2011). The latter model includes an RCP2.6 run whereas the former does not.

A key metric assessed in this study is the area-proportion of the Earth that exhibits positive or negative warming trends over a specified period. Results are mostly displayed for negative trends (cooling area-

proportion), but the specific choice does not matter as the warming and cooling proportions sum to 1 and each can be inferred from the other. We use gridded temperature data and count the area represented by grid cells exhibiting trends of each sign. We assess trends of a range of lengths from 5 years to 50 years to account for both short and longer term trend behaviour. The area-proportion of warming/cooling trends is compared here to the trend in global mean temperature. To reflect the fact that this trend is assessed over a set of finite size window lengths, we denote the magnitude of the trend by the term 'warming rate'. The warming rate can of course be negative too, indicating a negative temperature trend (cooling) over a period. The trend estimates are simple linear least squares estimates fitted to the data in each interval. The shortest trend lengths considered here (5 years and 15 years) are strongly influenced by natural internal variability of climate (Lewandowsky et al., 2015) and we do not mean to imply that the sign of warming rate has broader significance for such short term trends. While shorter period trends have been termed 'pauses' or 'hiatuses' in recent climate literature (Lewandowsky et al., 2016), there is little or no statistical evidence to show that the trends associated with the alleged 'pauses' are unusual (Lewandowsky et al., 2015; Rahmstorf et al., 2017), and they are not indicative of longer-term warming rates.

3. Results

3.1. Global mean warming rates

The magnitude (and sometimes sign) of global mean warming rates depends on the length of time used to estimate the trend. The warming rates for trends of length 15 and 30 years in GMST are shown in Fig. 3. For observations (black lines) the warming rate is variable (especially for 15-year trends) up to about 1970, and is then consistently positive and generally rising. We also calculated warming rates for 5-year trends (not shown). The 5-year warming rates are highly variable and display little trend over the observed period. Since warming rates (trends) are derivatives, they are sensitive to small differences between different datasets, even where the underlying time series (as in Fig. 1) are nearly identical (Risbey and Lewandowsky, 2017).

Fig. 3 also shows the warming rates for the CMIP5 multi-model ensemble mean. For the historical forcing runs through 2005 the CMIP5 ensemble mean warming rates roughly track those in observations. This is partly because the historical forcing runs contain the aerosol forcing for the observed large volcanic eruptions, which drive some of the trend response (Marotzke and Forster, 2015). The models are properly synchronised to these events. The model ensemble mean smooths out much of the variability present in individual models and this removes much of the internally generated variability on the trend time scales (Risbey et al., 2014). This tends to smooth out the ensemble mean warming rate relative to observations. For the RCP projection period in Fig. 3 the warming rates are much smoother (than in the historical forcing period) in the RCP2.6, RCP4.5, and RCP8.5 ensemble means. This is because the RCP scenarios focus on greenhouse gas forcing and do not contain episodic external forcing variation from volcanoes and other sources (Maher et al., 2014).

The warming rates for the RCP scenarios in Fig. 3 are similar for the first decade or two and then diverge substantially. The warming rate continues to increase through the 21st Century for RCP8.5, but reaches a maximum by around 2025 in RCP4.5 and declines back to near zero by the end of the century. The warming rate stabilizes back toward smaller values for the RCP4.5 scenario as greenhouse forcing starts to stabilize, but at a higher level of global mean temperature. For the RCP2.6 ensemble mean, the warming rate declines more rapidly back toward zero and is effectively there by 2050, consistent with the stabilisation of forcing for this scenario just prior to that.

The warming rates for trends of all lengths between 5 and 50 years are shown for observations in Fig. 4. A salient feature of this display is the progressive retreat of negative warming rates to shorter trend lengths (reduction in vertical extent of blue areas) over the instrumental record. Another feature is the prominence of positive warming rates for any trend longer than about 20 years. The warming rates (trends) are consistently significant ($p < .05$) once trend lengths exceed about 17 years (Lewandowsky et al., 2015).

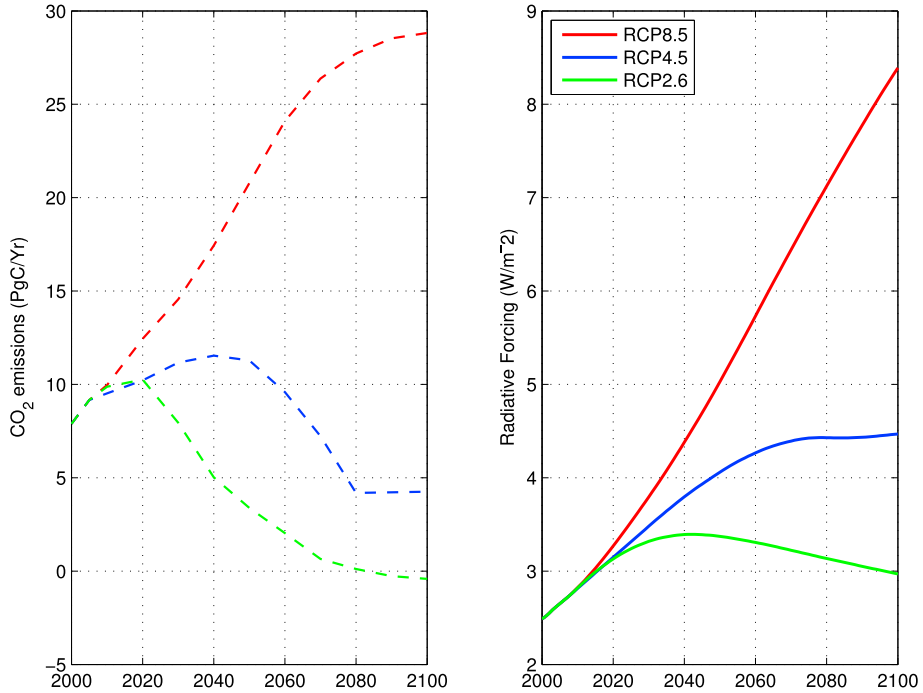

Fig. 2. The left panel shows CO_2 emissions under each of the scenarios RCP2.6 (green), RCP4.5 (blue) and RCP8.5 (red). The right panel shows the radiative forcing in W/m^2 for all greenhouse gases in scenarios RCP2.6 (green), RCP4.5 (blue) and RCP8.5 (red).

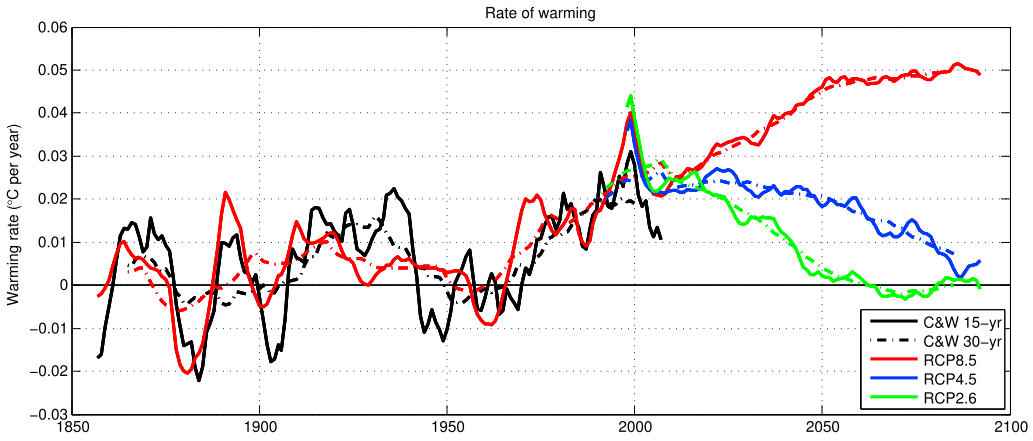

Fig. 3. Global mean warming rates defined as the magnitude of the linear trends for running 15-year trends (solid lines) and 30-year trends (dashed lines) of GMST. The black curve is Cowtan & Way data. The red curve to 2005 is the CMIP5 ensemble mean from the historical forcing runs. After 2005 the red curve is the CMIP5 RCP8.5 ensemble mean, the blue curve is the RCP4.5 ensemble mean and the green curve is the RCP2.6 ensemble mean. Each warming rate value is plotted at the central year of the time window used to calculate the trend.

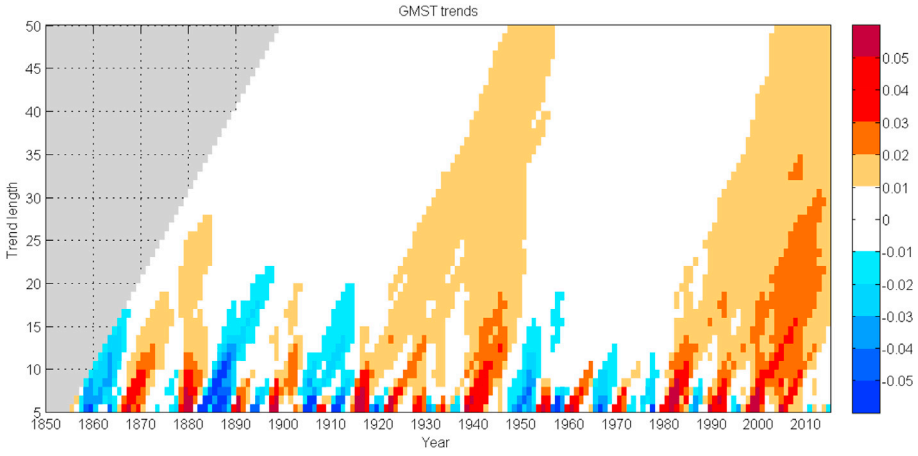

Fig. 4. Global mean warming rates (°C/year) defined as the magnitude of the linear trends as a function of the length of the trend (vertical axis) and the last year used to determine the trend (year axis). The data are Cowtan & Way. Note, the extreme outermost colour bar categories include all trends $\gtrless \pm 0.05$. Grey shading indicates no data.

3.2. Spatial variation in warming rates

All areas of the planet do not warm or cool at the same rate as the global mean. To assess spatial variation in the magnitude of the warming rate, we used gridded GMST data (Cowtan and Way, 2014) to calculate the rate of warming in each grid cell for trends of specified length (15 and 30 years). We then generate a histogram of the proportion of the area of the Earth with warming rates in each of a set of warming rate bins. An example of these histograms is shown for observations in Fig. 5a for a few selected 15-year periods. One period is selected centred on 1950 to characterise the period before modern greenhouse warming (Cahill et al., 2015; Lewandowsky et al., 2015) and another spans the recent 15-year

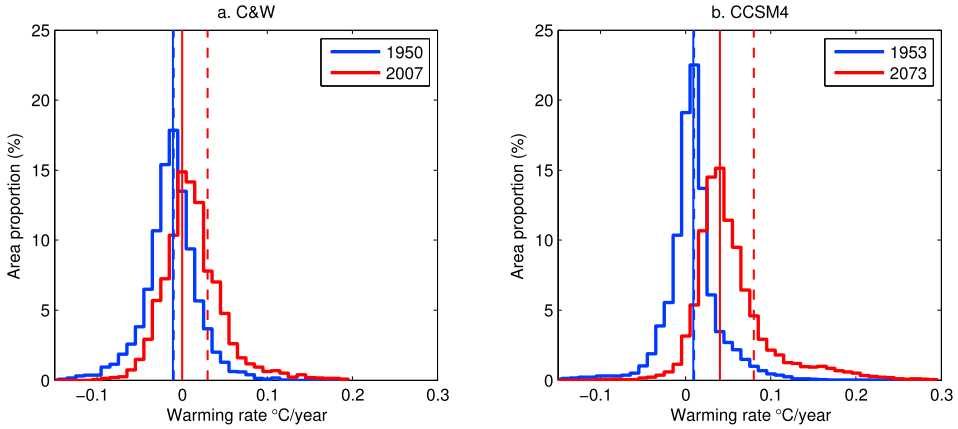

Fig. 5. Histograms showing the proportion of the area of Earth with 15-year warming rates in each warming rate bin spanning 0.01 °C/year for two example central years in a) Cowtan & Way gridded observations and b) the CCSM4 RCP8.5 run. The solid vertical lines mark the mode of the distributions and the dashed vertical lines mark the mean.

period of warming. The tendency illustrated by the example years is for the histogram to move to the right (span higher warming rates) and develop a warm tail (some areas emerge with extreme warming rates) as the global mean warming rate increases. This response is evident in observations by comparing the area-proportion histograms for centred years 1950 and 2007. This behaviour is further exemplified in histograms from the CCSM4 model RCP8.5 run in Fig. 5b, showing the fat tail typical of this high forcing run. From 1953 to 2073 the area-proportion histogram has shifted well to the right and exhibits a fat tail characterising some areas with extreme high warming rates.

To explore these tendencies in more detail, we calculate histograms for each centred year and show the percentage area of the Earth with trends in each magnitude range, running through time (Fig. 6). At the outer limit of these histograms (0.12 °C/year for 15-year trends and 0.08 °C/year for 30 year trends) we accumulate the percentage area with all trends greater than the histogram limit. That means that the top histogram bin is unbounded, but that allows us to track changes in the high and low tails. The modes of the area histograms (thin black line) trace out an evolution of warming rate that is similar to the series for the global mean warming rate in Fig. 3.

The vertical spread of the histograms at each point in time in Fig. 6 tells us how much variation in warming rate occurs in space. For the 15-year trends, the spread of warming rates across values that account for at least 2.5% of the area of the planet at the high and low warming rate ends of the distribution (the width spanned by the lightest colour shading) is large and in the vicinity of 0.1 °C/year. That spread accounts for why some areas can display cooling trends (−*ve* warming rates) even when the global mean warming rates are substantially positive. For the 30-year trends, the spread of warming rates spanning the 2.5% areas is typically about 0.05 °C/year, but may have broadened in range in the recent period.

In the most recent periods (post 1990) much of the area in the warming rate spread is associated with positive rates for both 15 and 30-year trends in Fig. 6. Further, there are indications that the high tail (proportion of areas warming faster than the specified upper tail limit, represented by coloured squares in the top row) is spreading to encompass warming rates without precedent in the instrumental record (Hansen et al., 2012; Rhines and Huybers, 2013; Stone et al., 2013). In the most recent period, more than 2.5% of the area of the planet is warming at rates more than 5 times the modal area warming rate values for 15-year trends, and more than 4 times the rate for 30-year trends. The areas predominantly contributing to this high warming rate tail in Fig. 6 are the Arctic and Greenland. This result is consistent with studies describing recent rapid warming in the Arctic (Serreze et al., 2009; Screen and Simmonds, 2010; Cowtan and Way, 2014).

An assessment of future changes in the proportion of areas with different warming rates is given in Fig. 7 for the CCSM4 model with RCP2.6, 4.5, and 8.5 forcing. For RCP8.5 the warming rates stay positive for almost all areas throughout the 21st century, and the occurrence of areas exceeding an upper warming rate of 0.15 °C/year in the high tail is common by the end of the century. For RCP 4.5 and 2.6, the median area warming rates return toward zero warming rate about the times the forcing is stabilised in each (2100 and 2050 respectively). The occurrence of 2.5% or more of the area above the high tail threshold also varies with scenario. For RCP4.5 there are some periods over the rest of the century where this occurs, but no further occurrences for RCP2.6.

Another indication of the spread of tail of areas with high warming rates is given in Figs. 6 and 7 by the divergence of the mode lines of the

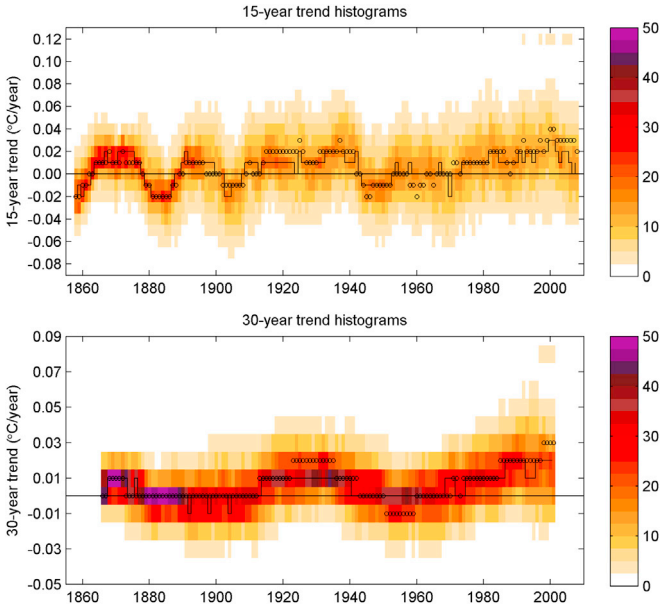

Fig. 6. Running histograms of the percentage area of the Earth with trend magnitudes falling into each histogram bin range for a) 15-year trends and b) 30-year trends. The histograms run vertically, with year on the x-axis corresponding to the central year of the trend window. In the tails of the histogram we expand the outer bin to include all warming rates greater/lesser than +0.12/−0.12 °C/year for 15-year trends and +0.08/−0.08 °C/year for 30-year trends. The colour bar corresponds to areal percentages for the amount of area showing trends in each discrete trend magnitude bin. Where a trend magnitude bin has area less than 2.5% it is shaded white. The thin black line denotes the mode of each histogram and the circles the mean. The data used are Cowtan & Way gridded observations.

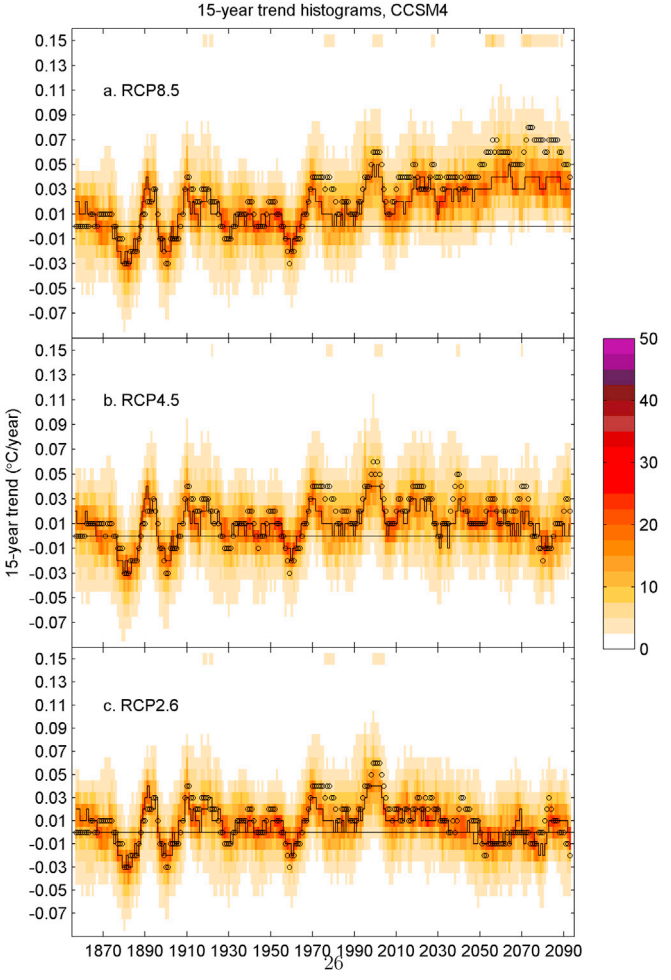

Fig. 7. As in Fig. 6, but for the CCSM4 model for 15-year trends for a) RCP8.5, b) RCP4.5, and c) RCP2.6. For CCSM4 the outer histogram bin includes all areas with warming rates greater/lesser than +0.15/−0.15 °C/year.

distributions (solid lines) and means (circles). For observations the mode and mean are usually colocated until the very recent period, where the higher mean value indicates the emergence of a skewed warmer tail. For the CCSM4 model area distributions in Fig. 7 the separation of the mean from the mode is particularly apparent toward the end of this century in the RCP8.5 run. This fat tail behaviour is illustrated by the histogram for the year 2073 in Fig. 5b. The highly non-Gaussian nature of the distribution in this scenario implies a climate more predisposed to regime transitions (Franzke et al., 2008, 2009; Lockwood, 2001; Drijfhout et al., 2015). A more detailed examination of the non-Gaussian character of the distribution is forthcoming.

3.3. Relationship between global mean warming rate and area-proportion

In a stationary climate that was neither warming nor cooling we might expect to see a roughly even proportion of the area of the planet displaying warming and cooling trends over time. In a non-stationary (warming) climate, these proportions should change through time. The rate at which the proportions change depends on the length of time over which the trends are assessed, the global rate of warming, and the degree to which the warming is uniformly spread across areas. If the warming were highly localised, then the area-proportion undergoing warming theoretically might not change much, and consequently there might not be a strong relationship between global mean warming rate and the proportional area showing warming.

One indication of this relationship is given in Fig. 6. If the increase in warming rate was highly localised, then we would see a shift in profile of the distribution of warming rates in this figure, with some regions moving from moderate to high warming rates. On the other hand, if nearly all regions warm, we would see an upward (warmer) shift in the whole distribution, while preserving its shape. There is some evidence of both of these responses in recent decades, meaning that a high tail emerges in the distribution and the whole distribution moves to faster warming rates.

To further test the degree to which changes in global mean warming rate are reflected by changes in the area-proportion showing warming/cooling trends, we plot the global mean warming rate against cooling area proportion in Fig. 8. This plot assesses warming trends over 5, 15, and 30-year periods. For example, for the 5-year trends, we assess the trend (°C/year) for each period of 5-year length GMST and the corresponding 5-year trends in each of the grid boxes in the gridded surface temperature data. The area-proportion is calculated from the area of grid boxes showing positive and negative trends.

For the 5-year trends (Fig. 8a) the scatter plot of GMST trend and area-proportion shows only a moderate relationship. That is perhaps not surprising as 5-year trends are dominated by natural variations (internal and forced) set by a range of different processes at both global and regional scale. As such, we would not expect strict correspondence between global internal variations and those occurring in different regions on this time scale. For the 15-year and 30-year trend lengths (Fig. 8b and c) the scatter plot shows a close relationship between global mean warming rate and the area-proportion in warming/cooling. That is, for trends of this length the warming rate in the global mean is a good predictor of the proportion of the Earth's area likely to be undergoing warming or cooling. This implies that when the global mean warming rate increases (warming accelerates), that occurs predominantly through an increase in the area showing positive warming rates, rather than by holding the area constant and increasing the rate of warming in localised areas already displaying warming.

We repeated the test of the relationship between global mean warming rate and the area-proportion showing warming/cooling for one of the CMIP5 models — ACCESS 1.0 (Dix & coauthors, 2013). The results are shown again for trends of length 5, 15, and 30 years in Fig. 9. In this case the overlap with observations is covered by the historical forcing in CMIP5 (to 2005) and is shown with black dots. For the period after 2005 we show results for both RCP4.5 forcing (blue) and RCP8.5 forcing (red).

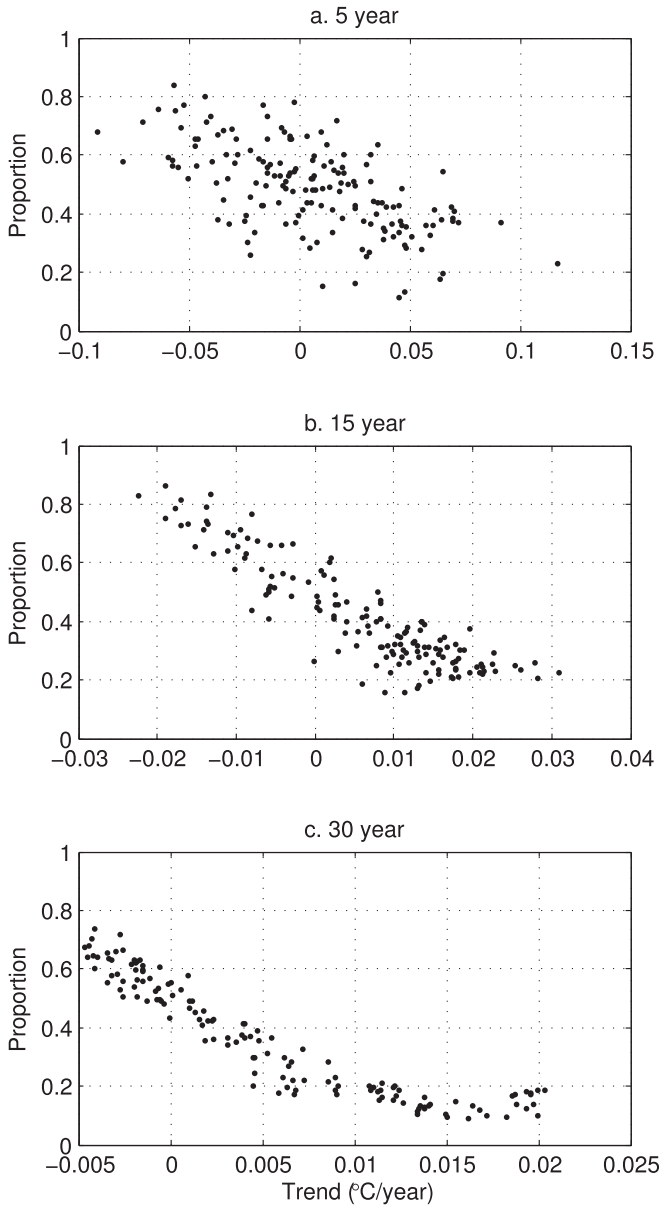

Fig. 8. Scatter plot of the area-proportion of the Earth with surface temperature trends <0 (negative) versus the magnitude of the global mean trend for trends of length a) 5-years, b) 15-years, and c) 30-years. The data are from Cowtan and Way observations spanning 1850–2015.

The model results for the historical period overlapping with observations (black dots) are qualitatively similar to those for the observations in Fig. 8. That is, for 5-year trends there is a moderate relationship, but for 15 and 30-year trends the relationship is strong. The model warming rates are similar to those in observations for each trend length, as is the variation in area-proportion.

For the RCP periods in the future, the global mean warming rates are typically higher than for the historical period (blue and red dots shifted to the right of the black dots in Fig. 9). For the ACCESS model results, the relationship between global mean warming rate and area-proportion is not linear. As warming rates increase, the area-proportion with cooling trends does not drop linearly to zero, but tends to asymptote toward it. Even when the planet is warming rapidly, there will still be some few areas showing negative trends.

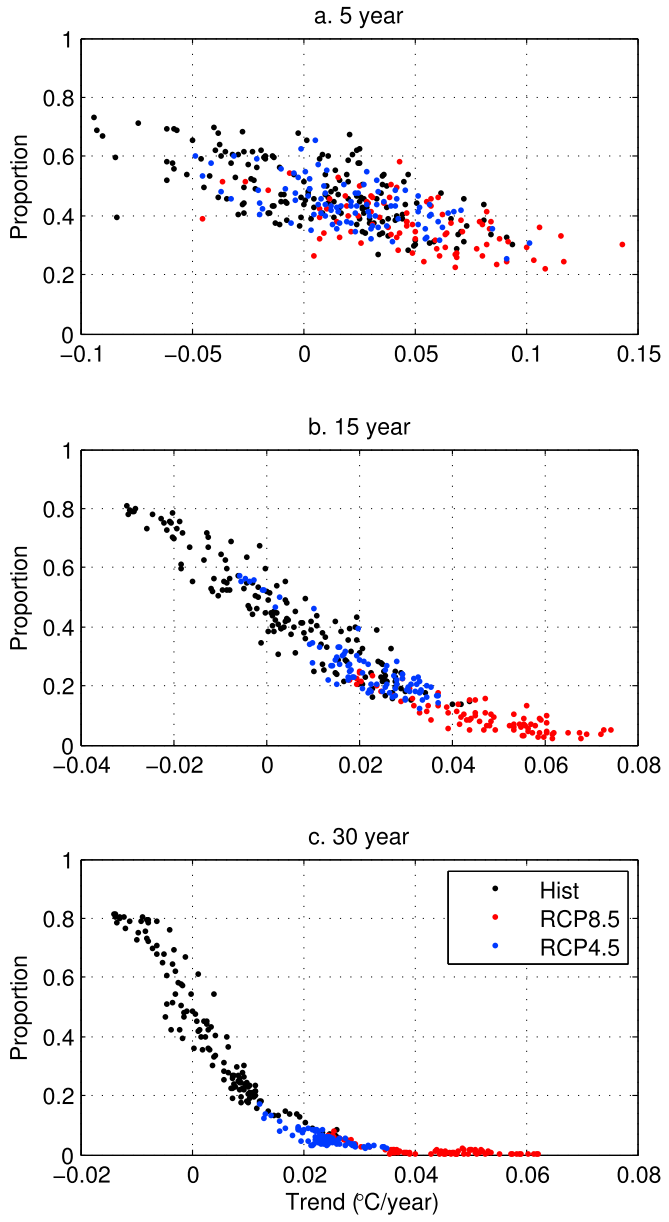

Fig. 9. As in Fig. 8, but for the ACCESS1.0 historical run (black), RCP4.5 (blue), and RCP8.5 (red).

3.4. Transient response of area-proportion

We have established thus far that the area-proportion of warming/cooling trends does reflect the global mean warming rate for trends of sufficient length. In this section we examine the temporal characteristics of the area-proportion for trends of different lengths. We expect the area-proportion to vary for the reasons given in section 1, but it ought also to be responding to the increase in warming rate. This behaviour is illustrated in Fig. 10, which shows the areal proportion of the Earth exhibiting negative GMST trends over periods of length 5, 15, and 30 years respectively. The 5-year trends are too short for the area-proportions to reflect the long term warming (Lewandowsky et al., 2015) and are less tightly related to the global mean warming rate (section 3.3). As such they display relatively little variation in the mean proportion trend in time through the instrumental period and through the RCP projections to 2100.

For the longer period trends (15 and 30 years) there is substantial variability in the proportions in the observational data through time in Fig. 10, with proportions varying between 20 and 80% of the area with negative GMST trends. The model ensemble envelope of proportional area appears reasonably well calibrated to the variations in the observational data. The model ensemble projections indicate a reduction in model spread in coming decades and a shift to cooling area proportions below the bottom of the historical range. Note that for the RCP4.5 scenario (blue ensemble in Fig. 10) the area-proportion recovers back toward even proportions by the end of the projection period (albeit at a much higher GMST ~2 °C above pre-industrial — see Fig. 1b). This is because the area-proportion depends on the rate of warming, not the amount, and the rate of global mean warming eventually reduces for the RCP4.5 run (Fig. 3).

In the recent observational period, up to 40% of the area of the planet exhibits negative 15-year trends, and up to 20% of the area exhibits negative 30-year trends. This is important in setting expectations (Grose et al., 2017). If one is in a region that is actually experiencing a negative multi-decadal trend in the face of long term global warming, that is not that unusual, as about a fifth of the planet is expected to do so.

It is further instructive to assess the proportional area exhibiting negative trends for trends of all possible lengths (up to 50 years) in the observational record. This result is shown in Fig. 11a. It is apparent here that for trend lengths of less than about 15 years, the preponderance of area in warming or cooling switches back and forth through time, favouring one, then the other. The Earth exhibits natural fluctuations in warming rate on these short time scales that are larger or comparable to the signal of climate change on this time scale (Lewandowsky et al., 2015; Risbey et al., 2015), so it is not surprising that large areas of the planet may exhibit warming or cooling on this time scale.

For trend lengths beyond about 30 years in Fig. 11a, the balance of the area-proportion mostly favours warming trends (red areas), particularly post 1920. For longer trends (beyond about 20 years) in the most recent observational period, the area of the planet displaying any cooling trend has dropped below 25%.

To assess the potential for any change in the trend toward smaller areas of the planet displaying cooling, we repeated the area assessment for observations in Fig. 11a with results from CMIP5 climate models with RCP8.5 forcing to 2100. The CMIP5 models are similar in their response to RCP8.5 in displaying widespread ongoing warming. We show typical results here for the ACCESS1.0 model in Fig. 11b. The model projects that the area-proportion showing negative trends continues to drop to below 5% of the area of the Earth for trends of 20-years and longer. This may be a slight over-estimate in that the RCP8.5 scenario does not contain any sustained negative forcings such as clusters of large volcanic eruptions, that can sometimes occur, inducing short-term negative trends (Maher et al., 2014). Nonetheless, the RCP8.5 projection suggests that it will become increasingly unlikely to find regions of the planet that are not warming on 20+ year time scales under this forcing scenario.

4. Conclusions

The global mean warming rate for trends of 15 years length varied positive (warming) and negative (cooling) over the instrumental record until about 1970. Thereafter, it has remained positive and generally increasing (with overlying variability) in observations. The projected changes in warming rates in the CMIP5 ensembles highlight the substantial role of emissions reductions in modifying future warming rates. For the RCP8.5 scenario where greenhouse forcing continues to increase over the 21st century, global mean warming rates also continue to increase to an average level of about 0.5 °C/decade by 2100. This warming rate and the temporal excursions about it would yield warming about 3–5 times faster than those that occur due to natural variations in the pre-greenhouse instrumental period for 15 and 30 year trends respectively. Such warming rates would place many species under stress (Quintero and Wiens, 2013; Oppenheimer et al., 2014). By contrast, for the RCP4.5 scenario where emissions reduce and greenhouse forcing stabilizes, the warming rates decline back toward zero as stabilisation is approached by 2100. That scenario offers potential eventual reprieve for species affected by the *rate* of warming, but not the *amount*, since the rate reduction

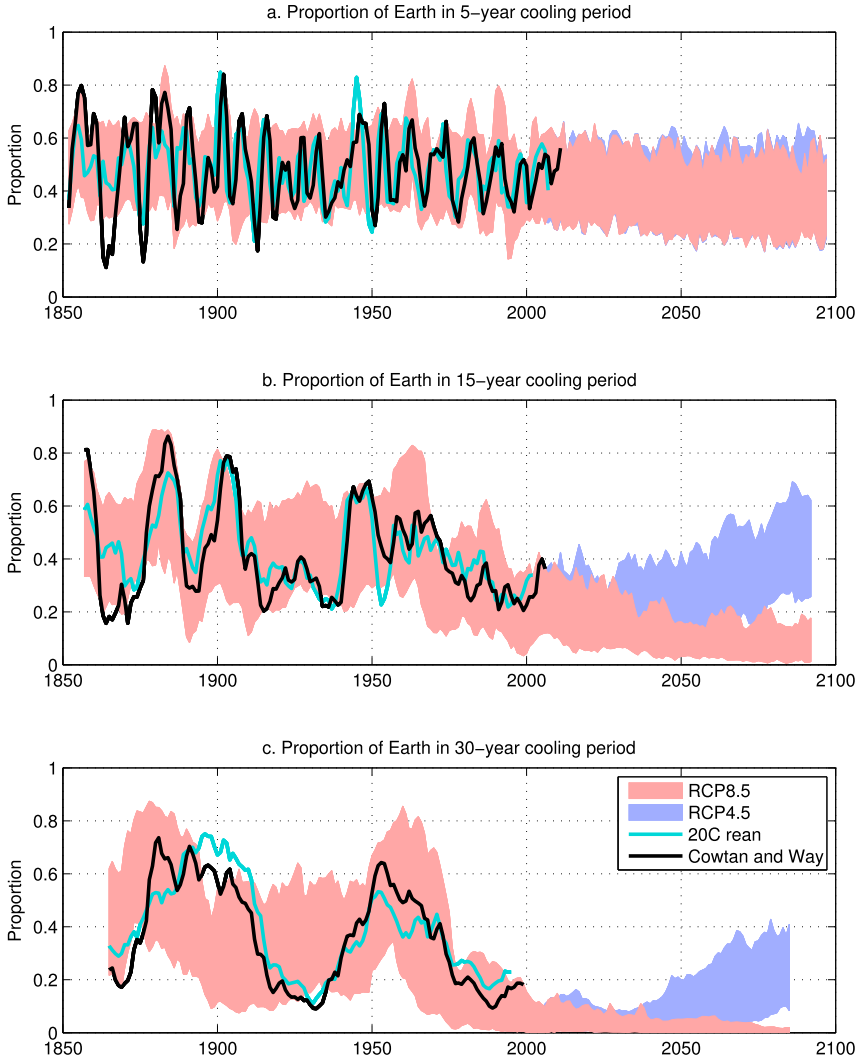

Fig. 10. The area-proportion of the Earth with GMST trends <0 (negative) for a) 5-year trends, b) 15-year trends, and c) 30-year trends. The black line is gridded Cowtan and Way data, the blue line is the 20th Century reanalysis, and the bands are the CMIP5 2.5–97.5 percentile ensemble ranges for RCP4.5 (blue) and RCP8.5 (red).

occurs at a warming likely over 2 °C above preindustrial temperatures. A faster reduction in warming rate is achieved in the RCP2.6 scenario, where forcing stabilizes before 2050 and global mean warming rates are accordingly near zero by then.

Warming rates are not spatially uniform and can vary from area to area by up to 1/0.5 °C/decade for 15/30-year trends. This variation accounts for the existence of cooling trends in some areas of the planet, even when the global mean warming rate is substantially positive. In recent decades warming rates across the planet have increased for the majority of areas, and the spatial distribution of warming rates shows an emerging high tail of warming rates for some areas, up to 4 times the median area warming rate. These responses are consistent with the roles of natural variability and greenhouse climate feedbacks. The natural processes that generate differences in warming rates across the planet continue to operate as the planet warms. All else being equal, global warming would produce a translation of the spatial distribution of warming rates to higher values of warming rate with the same distribution profile. This accords with the shift of the distribution of warming rates to span higher values of warming rate. On top of that change, we might also expect some regions to warm more rapidly than in the past because of local feedbacks in the climate system responding to enhanced greenhouse forcing. Such responses are expected in the Arctic and have been attributed to loss of sea ice (Serreze et al., 2009; Screen and Simmonds, 2010). Rapid warming in the Arctic is associated here with the emergence of a long tail of high warming rates in the spatial warming rate distribution. For model scenarios for the rest of the century, extreme high warming rates in the tail of the area distribution occur more frequently for RCP8.5 forcing, but are not evident again for RCP2.6 forcing in the model examined.

The increase in warming rate of global mean temperature is accompanied by an increase in the proportion of the area of the Earth exhibiting warming (rather than cooling) trends. The area-proportion has a direct relationship with the global mean warming rate, which is particularly strong for trend periods longer than about 15 years. The relationship is nonlinear for high warming rates such that there are still some areas not exhibiting warming trends at high warming rates. This presumably reflects the fact that many natural processes can produce regional cooling, and some of these still prevail in some (few) regions in a rapidly warming climate.

The proportion of the area of the Earth exhibiting warming or cooling trends also depends on the length of the trends considered. The average area-proportion in 5-year warming or cooling is close to even (0.5) and does not change much through time in observations, nor under RCP 4.5 and 8.5 forcing scenarios in future. That is to say, wherever you are on the planet, you are about as likely to experience a short term negative GMST trend as a positive one, and that fact bears little upon global scale longer term trends. For 15 and 30-year trends, the proportion of the area of the Earth showing negative trend varies substantially from decade to

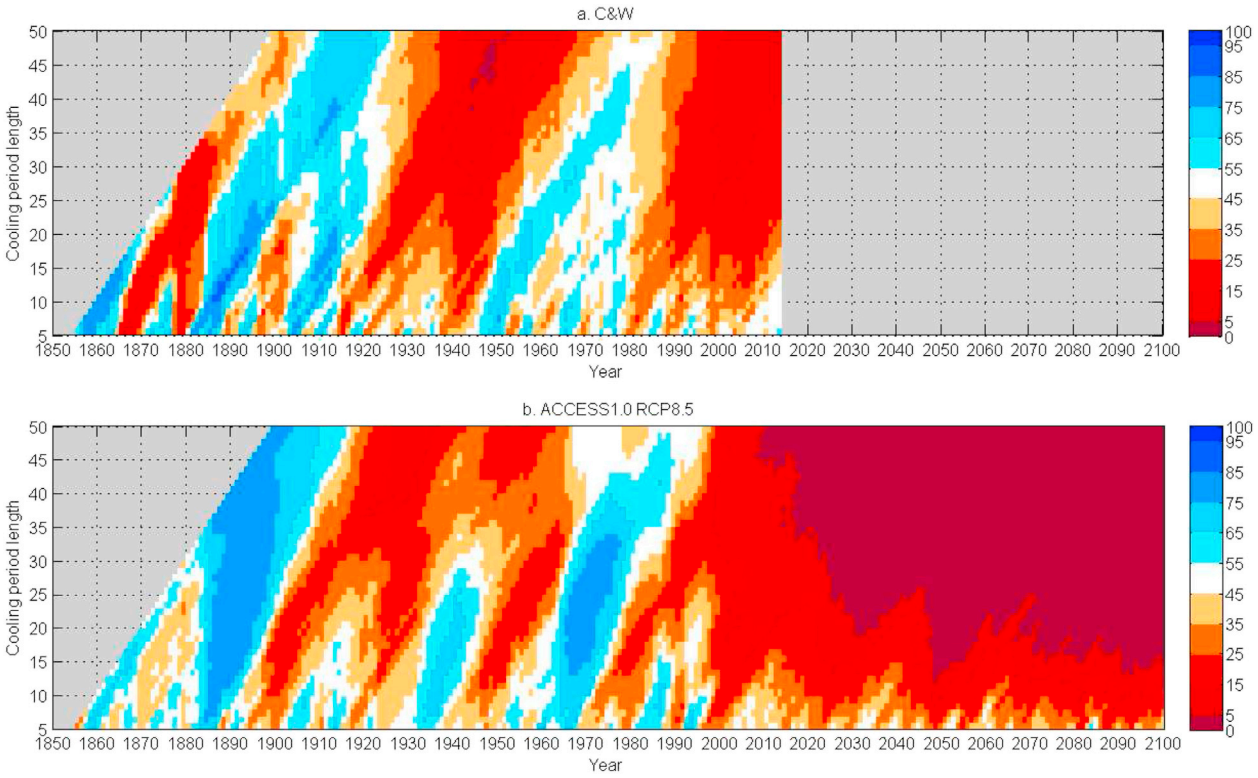

Fig. 11. The area percentage proportion of Earth with negative GMST trends as a function of the length of the trend (vertical axis) and the last year used to determine the trend (year axis) for a) Cowtan and Way gridded data and b) the ACCESS1.0 historical and RCP8.5 run. Red shading indicates dominance of warming trends and blue shading indicates dominance of cooling trends.

decade in observations, varying between about 0.2 and 0.8. This variation reflects the considerable decadal and multidecadal variability in GMST from internal processes and external forcing variations. For observations, the area-proportion with negative 15 and 30-year trends has dropped to the low end of the range in recent decades. For future decades, the CMIP5 RCP8.5 ensemble cooling area-proportion continues dropping toward small proportions. The RCP4.5 ensemble shows similar behaviour for a few decades and then starts to rebound as the RCP4.5 warming rates reduce.

In summary, global mean warming rates depend on the change in climate forcing, not the amount of forcing. Observations over the instrumental record have shown considerable temporal variation in global mean warming rates (from decade to decade), and considerable variation in the spatial distribution of that warming rate across the planet at any given point in time. In recent decades, the global mean warming rate is at its highest values in the instrumental period, and spatial variation in that rate is yielding some regions with warming rates of about 1 °C/decade. Reducing such extreme warming rates relatively quickly can be attained in the RCP2.6 scenario, but not the higher emission scenarios. For the high forcing scenarios the distribution of warming rates by area is highly skewed, indicating a less stable climate more prone to regime transitions.

Additional information

The authors declare no competing financial interests.

Acknowledgements

This work was funded by the CSIRO Decadal Forecasting Project (https://research.csiro.au/dfp), the Grains Research and Development Corporation, and the Earth Systems and Climate Change hub of the National Environmental Science Programme.

References

Burke, M., Hsiang, S., Miguel, E., 2015. Global non-linear effect of temperature on economic production. Nature 527, 235–239.
Cahill, N., Rahmstorf, S., Parnell, A., 2015. Change points of global temperature. Environ. Res. Lett. 10, 1–6.
Compo, G., Whitaker, J., Sardeshmukh, P., Matsui, N., Allan, R., Yin, X., Gleason, B., Vose, R., Rutledge, G., Bessemoulin, P., Brönnimann, S., Brunet, M., Crouthamel, R., Grant, A., Groisman, P., Jones, P., Kruk, M., Kruger, A., Marshall, G., Maugeri, M., Mok, H., Nordli, O., Ross, T., Trigo, R., Wang, X., Woodruff, S., Worley, S., 2011. The twentieth century reanalysis project. Q. J. R. Meteor. Soc. 137, 1–28.
Cowtan, K., Hausfather, Z., Hawkins, E., Jacobs, P., Mann, M., Miller, S., Steinman, B., Stolpe, M., Way, R., 2015. Robust comparison of climate models with observations using blended land air and ocean sea surface temperatures. Geophys. Res. Lett. 42, 6526–6534.
Cowtan, K., Way, R., 2014. Coverage bias in the HadCRUT4 temperature series and its impact on recent temperature trends. Q. J. R. Meteor. Soc. 140, 1935–1944.
Dix, M., coauthors, 2013. The ACCESS coupled model: description, control climate and evaluation. Aust. Meteorol. Ocn. J. 63, 9–32.
Drijfhout, S., Bathiany, S., Beaulieu, C., Brovkin, V., Claussen, M., Huntingford, C., Scheffer, M., Sgubin, G., Swingedouw, D., 2015. Catalogue of abrupt shifts in intergovernmental panel on climate change climate models. Proc. Natl. Acad. Sci. U. S. A. 112, 5777–5786.
Franzke, C., Crommelin, D., Fischer, A., Majda, A., 2008. A hidden Markov model perspective on regimes and metastability in atmospheric flows. J. Clim. 21, 1740–1757.
Franzke, C., Horenko, I., Majda, A., Klein, R., 2009. Systematic metastable atmospheric regime identification in an AGCM. J. Atmos. Sci. 66, 1997–2012.
Gent, P., Danabasoglu, G., Donner, L., Holland, M., Hunke, E., Jayne, S., Lawrence, D., Neale, R., Rasch, P., Vertenstein, M., Worley, P., Yang, Z., Zhang, M., 2011. The community climate system model version 4. J. Clim. 24, 4973–4991.
Grenier, P., de Elia, R., Chaumont, D., 2015. Chances of short-term cooling estimated from a selection of CMIP5-based climate scenarios during 2006–35 over Canada. J. Clim. 28, 3232–3249.
Grose, M., Risbey, J., Whetton, P., 2017. Tracking regional temperature projections from the early 1990s in light of variations in regional warming, including warming holes. Clim. Change 140, 307–322.
Hansen, J., Ruedy, R., Sato, M., Lo, K., 2010. Global surface temperature change. Rev. Geophys. 48, 1–29.
Hansen, J., Sato, M., Ruedy, R., 2012. Perception of climate change. Proc. Natl. Acad. Sci. U. S. A. 109, E2415–E2423.
Hansen, J., Takahashi, T., 1984. Climate processes and climate sensitivity. AGU Geophys. Monogr. 29, 1–32.

Hausfather, Z., Cowtan, K., Clarke, D., Jacobs, P., Richardson, M., Rohde, R., 2017. Assessing recent warming using instrumentally homogeneous sea surface temperature records. Sci. Adv. 3, 1–13.
Held, I., 1993. Large-scale dynamics and global warming. Bull. Amer. Met. Soc. 74, 228–241.
Houghton, J.T., Jenkins, G., Ephraums, J. (Eds.), 1990. Climate Change: the IPCC Scientific Assessment. Cambridge Univ. Press, Cambridge, UK, p. 365.
Kent, E., et al., 2017. A call for new approaches to quantifying biases in observations of sea-surface temperature. Bull. Amer. Met. Soc. 98 (8), 1601–1616.
Kobayashi, S., Ota, Y., Harada, Y., Ebita, A., Moriya, M., Onoda, H., Onogi, K., Kamahori, H., Kobayashi, C., Endo, H., Miyaoka, K., Takahashi, K., 2015. The JRA-55 reanalysis: general specifications and basic characteristics. J. Met. Soc. Jpn. 93, 5–48.
Lewandowsky, S., Risbey, J., Oreskes, N., 2015. On the definition and identifiability of the alleged "hiatus" in global warming. Sci. Rep. 5, 1–12.
Lewandowsky, S., Risbey, J., Oreskes, N., 2016. The 'pause' in global warming: turning a routine fluctuation into a problem for science. Bull. Amer. Met. Soc. 97, 723–733.
Lockwood, J., 2001. Abrupt and sudden climatic transitions and fluctuations: a review. Int. J. Climatol. 21, 1153–1179.
Maher, N., Sen Gupta, A., England, M., 2014. Drivers of decadal hiatus periods in the 20th and 21st centuries. Geophys. Res. Lett. 41, 5978–5986.
Marotzke, J., Forster, P., 2015. Forcing, feedback, and internal variability in global temperature trends. Nature 517, 565–570.
Morice, C., Kennedy, J., Rayner, N., Jones, P., 2012. Quantifying uncertainties in global and regional temperature change using an ensemble of observational estimates: the HadCRUT4 data set. J. Geophys. Res. 117, 1–22.
Moss, R., et al., 2010. The next generation of scenarios for climate change research and assessment. Nature 463, 747–756.
O'Kane, T., Risbey, J., Franzke, C., Horenko, I., Monselesan, D., 2013. Changes in the meta-stability of the mid-latitude Southern Hemisphere circulation and the utility of non-stationary cluster analysis and split flow blocking indices as diagnostic tools. J. Atmos. Sci. 70, 824–842.
O'Kane, T., Risbey, J., Monselesan, D., Horenko, I., Franzke, C., 2016. On the dynamics of persistent states and their secular trends in the waveguides of the Southern Hemisphere troposphere. Clim. Dynam. 46, 3567–3597.
Oppenheimer, M., Campos, M., Warren, R., Birkmann, J., Luber, G., O'Neill, B., Takahashi, K., 2014. Emergent risks and key vulnerabilities. In: Climate Change 2014: Impacts, Adaptation, and Vulnerability. Cambridge Univ. Press, Cambridge, UK, p. 1820 (chapter 19). (pp. 1039–1099).
Quintero, I., Wiens, J., 2013. Rates of projected climate change dramatically exceed past rates of climatic niche evolution among vertebrate species. Eco. Let. 16, 1095–1103.
Rahmstorf, S., Foster, G., Cahill, N., 2017. Global temperature evolution: recent trends and some pitfalls. Environ. Res. Lett. 12, 1–7.
Ramanathan, V., Callis, L., Cess, R., Hansen, J., Isaksen, I., Kuhn, W., Lacis, A., Luther, F., Mahlman, J., Reck, R., Schlesinger, M., 1987. Climate-chemical interactions and effects of changing atmospheric trace gases. Rev. Geophys. 25, 1441–1482.
Ramaswamy, V., et al., 2001. Radiative forcing of climate change. In: Climate Change 2001: the Scientific Basis. Cambridge Univ. Press, Cambridge, UK, p. 881 (chapter 6). (pp. 349–416).
Rhines, A., Huybers, P., 2013. Frequent summer temperature extremes reflect changes in the mean, not the variance. Proc. Natl. Acad. Sci. U. S. A. 110, E546.
Risbey, J., 2015. Free and forced climate variations. Nature 517, 562–563.
Risbey, J., Lewandowsky, S., 2017. The 'pause' unpacked. Nature 545, 37–39.
Risbey, J., Lewandowsky, S., Hunter, J., Monselesan, D., 2015. Betting strategies on fluctuations in the transient response of greenhouse warming. Philos. Trans. R. Soc. A 373, 14–27.
Risbey, J., Lewandowsky, S., Langlais, C., Monselesan, D., O'Kane, T., Oreskes, N., 2014. Well-estimated global surface warming in climate projections selected for ENSO phase. Nat. Clim. Change 4, 835–840.
Schneider, S.H., Thompson, S., 1981. Atmospheric co_2 and climate: importance of the transient response. J. Geophys. Res. 86, 3135–3147.
Screen, J., Simmonds, I., 2010. The central role of diminishing sea ice in recent Arctic temperature amplification. Nature 464, 1334–1337.
Serreze, M., Barrett, A., Stroeve, J., Kindig, D., Hilland, M., 2009. The emergence of surface-based Arctic amplification. Cryosphere 3, 11–19.
Stocker, T., et al., 2013. Technical summary. In: Climate Change 2013: the Physical Science Basis. Contribution of Working Group I to the Fifth Assessment Report of the Intergovernmental Panel on Climate Change. Cambridge Univ. Press, Cambridge, UK, p. 1535 (pp. 33–115).
Stone, D., Paciorek, C., Pall, P., Wehner, M., 2013. Inferring the anthropogenic contribution to local temperature extremes. Proc. Natl. Acad. Sci. U. S. A. 110, E1543.
Sutton, R., Suckling, E., Hawkins, E., 2015. What does global mean temperature tell us about local climate. Philos. Trans. R. Soc. A 373, 1–14.
Taylor, K., Stouffer, R., Meehl, G., 2012. An overview of CMIP5 and the experiment design. Bull. Amer. Met. Soc. 93, 485–498.
Thomas, C., Cameron, A., Green, R., Bakkenes, M., Beaumont, L., Collingham, Y., Erasmus, B., Siqueira, M., Grainger, A., Hannah, L., Hughes, L., Huntley, B., Jaarsveld, A.V., Midgley, G., Miles, L., Ortega-Huerta, M., Peterson, A., Phillips, O., Williams, S., 2004. Extinction risk from climate change. Nature 427, 145–148.